

Contents flfists avafiflabfle at ScfienceDfirect

### Ufltramficroscopy

journal homepage: www.elsevier.com/locate/ultramic



# A reference-area-free strafin mappfing method usfing precessfion eflectron dfiffractfion data

Dexfin Zhao <sup>a,1</sup>, Anfiket Patefl <sup>a,1</sup>, Aaron Barbosa <sup>a</sup>, Marcus H. Hansen <sup>a</sup>, Afinfiu L. Wang <sup>a</sup>, Jfiaqfi Dong <sup>a</sup>, Yuwefi Zhang <sup>b</sup>, Tejas Umafle <sup>a</sup>, Ibrahfim Karaman <sup>a</sup>, Patrfick Shamberger <sup>a</sup>, Sarbaifit Banerjee <sup>c</sup>, Matt Pharr <sup>b</sup>, Keflvfin Y. Xfie <sup>a,\*</sup>

- <sup>a</sup> Department of Materfials Scfience and Engineering, Texas A&M University, College Station, TX 77843, USA
- <sup>b</sup> Department of Mechanfical Engineering, Texas A&M Unfiversity, College Station, TX 77843, USA
- <sup>c</sup> Department of Chemfistry, Texas A&M Unfiversfity, College Statfion, TX 77843, USA

### ARTICLE INFO

Keywords:
Strafin mappfing
Precessfion effectron dfiffractfion (PED)
Denofise
VO<sub>2</sub>
Shape memory affloys (SMA)

#### ABSTRACT

In this work, we developed a method using precession effectron diffraction data to map the residual eflastic strafin at the nano-scalle. The diffraction pattern of each pfixel was ffirst collected and denofised. Tempflate matching was then appflied using the center spot as the mask to fidentify the positions of the diffraction disks. Statistics of distances between the seflected diffracted disks enable the user to make an finformed decision on the reference and to generate strafin maps. Strafin mappfing on an unstrafined stingle crystall sapphire shows the standard devitation of strafin measurement is 0.5%. With this method, we were abile to successfulfly measure and map the residual eflastic strafin in VO $_2$  on sapphire and martensite fin a Nfi $_{50.3}$ Tfi $_{29.7}$ Hf $_{20}$  shape memory affloy. This approach does not require the user to seflect a "strafin-free area" as a reference and can work on datasets even with the crystalls oriented away from zone axes. This method is expected to provide a robust and more accessible alternative means of studyfing the residual strafin of various material systems that compflements the existing afgorithms for strafin mappfing.

### 1. Introduction

Stored eflastfic strafin has a profound fimpact on the mechanficafl properties and functionalfitties of materiials. For exampfle, compressive residual stresses fin metals and ceramfics can suppress crack propagation, thereby fimproving the fracture toughness [1,2]. Residual eflastfic strafin can also affect band gaps, eflectron transport, and phonon transport [3–5]. X-ray diffiraction and neutron diffiraction are two popular techniques to measure and map the residual strafin fin materials [6,7]. Since both x-ray and neutron beams are difficult to focus, the residual strafin mappling using these two techniques has flimfited spatial resoflution.

To achfieve nanometer-scafle resoflution strafin mappfing, transmission effectron mficroscopy (TEM) and effectron diffiraction have been empfloyed. Effectrons are charged particfles, and thus effectron beam can be focused by tunfing the strength of the effectromagnetic flenses fin TEM. The effastfic strafin can be calculated from hfigh-resoflution TEM (HRTEM) mficrographs fin reafl space or by analyzing diffraction pattern

finformatfion fin recfiprocall space [8,9]. For the reafl-space fimaging mode, geometrfic phase anaflysfis (GPA) fis wfidefly used [10,11]. Aflthough qufite powerfufl, GPA can onfly be used on HRTEM mficrographs, fin which the phase contrast fis domfinant; fit cannot be appflied on regullar bright-ffield (BF) TEM fimages, where flattfice frfinges are absent. Hence, GPA has hfigh spatfiafl resoflution but a flfimfited ffield of vfiew (typficaflfly fless than or approxfimatefly 20×20 nm²).

In diffraction mode, Zuo and Spence pfioneered the work using convergent-beam eflectron diffraction (CBED) to obtain the strafin finformation and automate the process [12,13]. In the CBED patterns, flattice strafin can be precisely measured by trackfing the positions of higher-order Laue zone (HOLZ) flines fin the bright-ffield CBED dfisk [14, 15]. This approach works because HOLZ flines result from high-order reflections, which are very sensitive to changes fin the flattice spacfing [9]. By comparing the experimentality acquired HOLZ fline positions to computer stimuflattions, strafin finformation with high precision (approximately 0.2%) can be obtained [16,17].

E-mafil address: keflvfin.xfie@tamu.edu (K.Y. Xfie).

<sup>\*</sup> Correspondfing author.

<sup>&</sup>lt;sup>1</sup> These authors contributed equalify to this work.

Wfith the advent of 4D-STEM [18,19] and precessfion effectron dfiffractfion (PED) [20,21], a more computatfionaflfly cost-effectfive way to perform strafin mappfing fis to raster the beam on the specfimen, acqufire the dfiffractfion pattern at each pfixefl, and measure the shfifts of dfiffractfion spots for each pfixefl reflatfive to a reference pattern. PED combfines beam precessfion (the beam fistfiflted and rotated about the optficafl axfis at a very hfigh frequency, typficaflfly 100 Hz) wfith nanobeam dfiffractfion and offers a number of advantages fin performfing strafin mappfing compared to 4D-STEM. Ffirst, PED averages out the dynamficafl effects fin eflectron dfiffractfion, fleadfing to more unfiform dfiffractfion spot fintensfity and easfier spot center fidentfifficatfion [22,23]. In contrast, 4D-STEM utfiffizes CBED patterns, and the fiflflumfination fin the dfiffraction dfisks fis non-unfiform; the dfisk center fidentfifficatfion usuaflfly finvoflves the use of specfiaflfly patterned apertures or addfitfionafl reconstructfion steps [24-28]. Second, PED excfites hfigher-order refflectfions, whfich are more sensfitfive to changes fin flattfice parameter [8].

The current strafin mappfing methods used by 4D-STEM and PED share very sfinfiflar aflgorfithms [29,30]. The specfimen fis tfiflted to a flow-findex zone, and a "strafin-free" reference pattern fis acquired. Two non-coflflfinear dfiffractfion spots are then seflected to create the two non-coflflfinear vectors,  $g_1$  and  $g_2$ . The coordfinates of the two vectors fin the reference dfiffractfion can be expressed as the reference dfiffractfion matrfix  $G_0 = (g_{x1} \ g_{x2} \ g_{y1} \ g_{y2})$ . The two vectors fin the dfiffractfion pattern for strafin caflcuflatfion can be expressed finthe same way as the dfiffractfion matrfix G. The dfistortfion matrfix G hence can be sfimpfly expressed as  $G = (G_0 G^{-1})^t$ , where G is the transpose of the matrfix. The dfistortfion matrfix can be further decomposed finto a pure deformation matrfix and rotatfion matrfix to generate finformation of G into a pure deformation matrfix and rotatfion matrfix to generate strafin maps at nanometer and submficron scafle from both 4D-STEM and PED datasets [24,29,31–37].

We reaffize two features of the above aflgorfithm may ffinfit fits wfider appflication of strafin mappfing. Ffirst, a reference area fis required. In many cases, fit fis dfifficult to fidentify the appropriate "strafin-free" dfiffraction pattern, and fits seflection can be user-dependent and flackling the support of quantitative data. This shortcomfing fis particularly fimportant fin materials that contain high density of dfisflocations (e.g., martensfite grafins or heavifyl deformed grafins) and nanocrystafflifine sampfles, fin which an un-strafined prfistfine area fis dfifficult to ffind. Second, the aflgorfithm requires the sampfle to be tiflted to a flow-findex zone axis so that two non-coffinear vectors can be drawn. If the sampfle fis at a two-beam condition, the above aflgorfithm would faffil to work. In this flight, we developed a new PED-based strafin mappfing aflgorfithm that does not refly on the seflection of the reference dfiffraction pattern and can aflso work even when the sampfle fis not triflted to a flow-findex zone axis.

### 2. Materials and methods

Dfiffractfion patterns were obtafined wfith a 200 kV FEI Tecnafi F20 ST TEM equfipped wfith a ffield emfissfion gun. A NanoMEGAS ASTAR unfit was used to produce precessfion and descannfing of the eflectron beam. The spot sfize of the eflectron beam wfith a  $0.3^{\circ}$  precessfion angfle fis approxfimatefly 3 nm. AfIl dfiffractfion patterns were acqufired fin the fimages wfith  $580 \times 580$  pfixell resofluttion.

A VO $_2$  thfin ffifm deposfited on a c-cut sfingfle crystafl sapphfire substrate and a Nfi $_{50.3}$ Tfi $_{29.7}$ Hf $_{20}$  shape memory aflfloy (SMA) were used as modefl materfiafls. The growth of VO $_2$  on [0001] sapphfire fis hfighfly epfitaxfiafl, and thus resfiduafl strafin fis expected near the finterface [38]. The Nfi $_{50.3}$ Tfi $_{29.7}$ Hf $_{20}$  shape memory aflfloy fis martensfitfic at room temperature [39], and eflastfic strafin fis expected to be stored fin the materfiafl durfing the austenfite to martensfite transformatfion. VO $_2$  deposfitfion was achfieved by sputterfing from a pure V target usfing a pressure of 2.0 mTorr wfith a mfixture of argon and oxygen gas (Ar: 20 sccm, O $_2$ : 4.1 sccm) and a DC power of 200 W at 600  $^{\circ}$ C for 30 mfin then anneafled fin the chamber for another 30 mfin. Cross-sectfionafl TEM specfimens were prepared usfing a Thermo-Ffisher Heflfios G4 focused-fion beam (FIB). The Nfi $_{50.3}$ Tfi $_{29.7}$ Hf $_{20}$ 

SMA was produced by high vacuum finduction meflting of high purfity Nfi, Tfi, and Hf. The sampfle was then soflution treated to achieve a precipifitate-free microstructure. The TEM specimens were prepared from 3 mm dfisks and eflectropoflished using a Tenupofl-5 poflishing system with a soflution of 30% nfitric actid fin ethanofl at 40 °C to create eflectron transparent areas. More detaifled microstructural finformation on the SMA can be found fin our earlier work [40].

### 3. Results and discussion

### 3.1. Archfitecture of the algorfithm

The strafin mappfing aflgorfithm was wrfitten fin Python and consfists of flive steps. The workflow fis shown fin Ffig. 1. Ffirst, fit reads the .bflo ffife usfing HyperSpy [41]. Second, the user can seflect a ffifter (Gaussfian, non-flocafl means, or Wfiener) to denofise the dfiffractfion patterns for each pfixefl. Thfird, the center dfiffractfion dfisk fis used as a tempflate to fidentify the posfitfions of other dfiffracted beam dfisks usfing a correflatfion coeffficient cutoff (0.87 fin the defauflt settfing). Fourth, the user wffflseflect two dfiffractfion dfisks of finterest. The aflgorfithm wffflgo through aftldfiffractfion patterns, caflcuflate the dfistance of the seflected dfisks, and generate a dfistance hfistogram. Note the dfistance fis measured fin recfiprocafl space, and the unfit fis pfixefl. Ffinaflfly, the user wfffl determfine a "strafin-free dfistance" based on the dfistance hfistogram, and the aflgorfithm wfffl create the "strafin heat map".

### 3.2. Function of each step of the algorithm

In the ffirst step, HyperSpy, which is an open-source multifi-dimensional data analysis package, was used to read and open the .bflo fifle (generated by the *NanoMEGAS* PED system) fin the *Python* environment [41].

The second step afims to denofise the dfiffractfion patterns, and fits fimportance wffIlbe eflucfidated fin the thfird step shortfly. The dfiffractfion pattern shown finFfig. 2 was acqufired from a sfingfle crystafl sapphfire tfiflted to the  $[1)\overline{2}10]$  zone axfis. In the as-acqufired condfitfion, the dfiffractfion patterns are nofisy (Ffig. 2a), and background can be descrfibed as Pofisson nofise [42]. The fuzzy nofise fis better reveafled by the cflose-up vfiews of the center dfisk (red boxed regfion) and a dfiffracted dfisk (bflue boxed regfion). The nofise fis aflso fiflflustrated as hfigh-frequency spfikes fin the correspondfing 3D fintensfity proffifles.

One "brute-force" way to fimprove the sfignafl-to-nofise ratfio fis to fincrease the acqufisfitfion tfime of the dfiffractfion pattern at each pfixefl. However, this approach would flead to proflonged acqufisfitfion tfime and

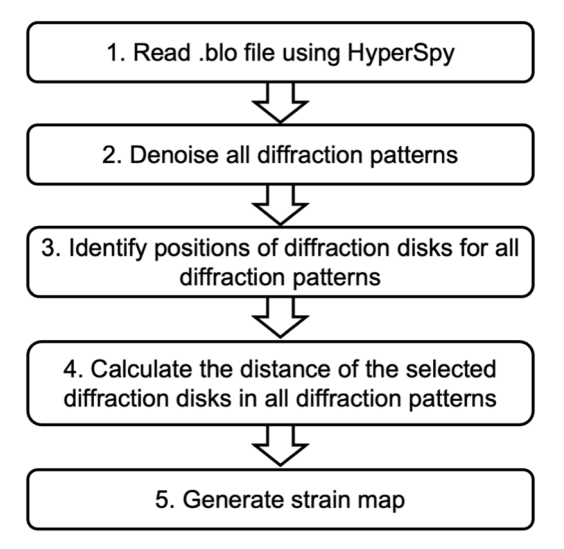


Fig. 1. Fflowchart describfing the key steps of the strafin mappfing aflgorfithm.

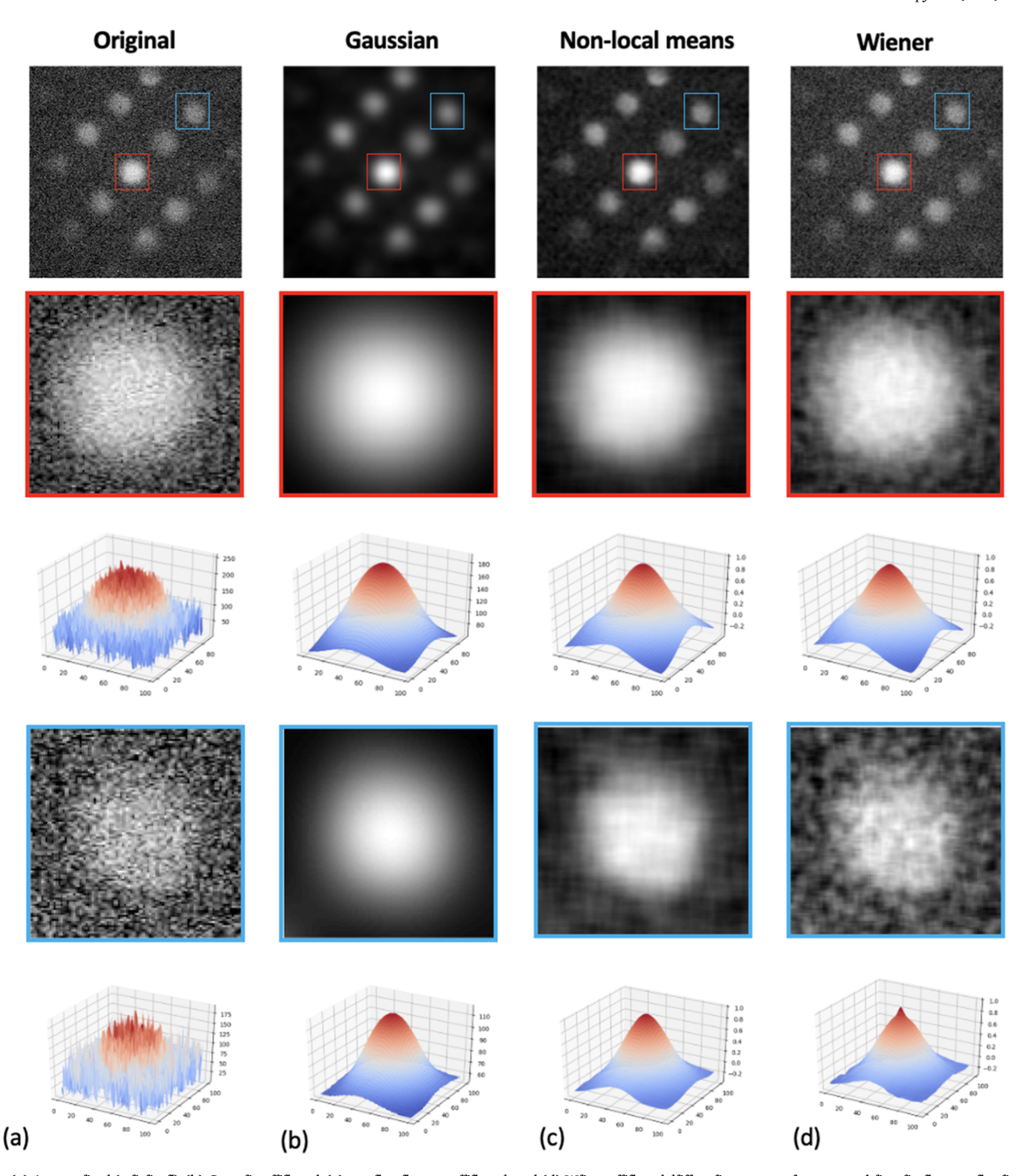


Fig. 2. (a) As-acquired (orfigfinafl), (b) Gaussfian ffifltered, (c) non-flocal means ffifltered, and (d) Wfiener ffifltered dfiffractfion pattern from a sapphfire stingle crystafl orfiented to the [1210] zone axfis. The red boxed and bflue boxed regfions are zoomed-fin vfiews of the dfirect beam and a dfiffracted dfisk, respectively. The corresponding 3D fintensity proffiles are aflso presented. (For finterpretation of the references to coflor fin this ffigure flegend, the reader is referred to the web version of this article.)

may resuflt fin damage to beam-sensfitfive sampfles. An aflternatfive way to reduce the nofise fis to appfly fimage ffiflters. Here, three common fimage ffiflters [24,42] were appflied: a Gaussfian ffiflter ( $\sigma=1.15$ ), a non-flocafl means ffiflter ( $\sigma=1.15$ , patch sfize = 3, and patch dfistance = 6), and a Wfiener ffiflter sfize = 5 and nofise power = 5). Note that the ffine detafifls of the ffiflters can be tuned by users. The nofise flevefl has reduced substantfiaflfly after appflyfing the ffiflters fin affl three cases, as shown fin Ffig. 2b-d. In partficuflar, the 3D fintensfity pflots of the center and dfiffracted dfisks exhfibfit smooth proffifles, conffirmfing the success of denofisfing from

the fimage ffiflters.

In the thfird step, the center dfisk was used as the tempflate to fidentify the posfitfion of dfiffracted dfisks. In this work, we used a correflatfion coeffficient of 0.87 as the cutoff for tempflate matchfing [43], and the user can choose a dfifferent vaflue. The fidentfiffied dfiffractfion dfisk posfitfions are marked by red dots fin Ffig. 3. In the orfigfinafl unffifltered fimage (Ffig. 3a), onfly the center spot was fidentfiffied as fitseflf was used as the tempflate. Dfisk posfitfion fidentfifficatfion was drastficaflfly fimproved wfith the denofise step. Mufltfipfle dfiffracted dfisks were recognfized fin the Gaussfian ffifltered

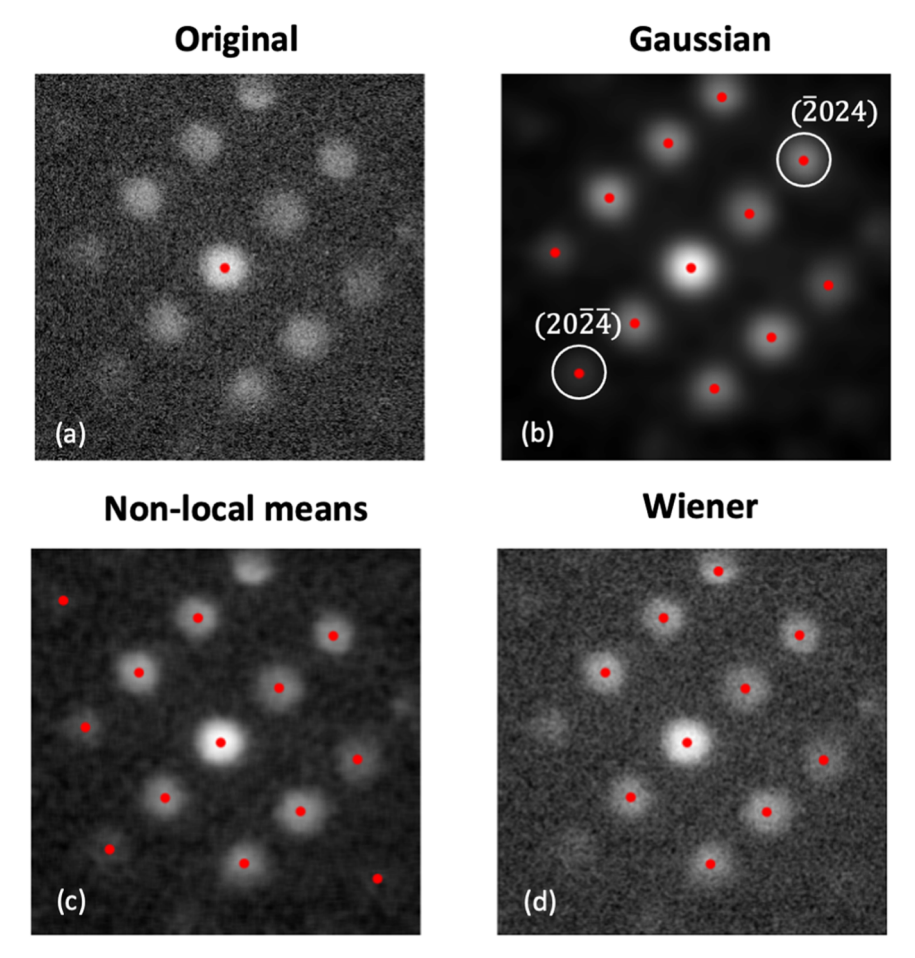


Fig. 3. Dfiffraction dfisk postition fidentfiffication using the dfirect beam as the mask fin the (a) orfigfinall, (b) Gaussian ffiltered, (c) non-flocall means ffiltered, and (d) Whener ffiltered dfiffraction patterns. Red dots findficate the postition of fidentfiffied dfisks. (For finterpretation of the references to coflor fin this ffigure flegend, the reader fix referred to the web version of this article.).

(Ffig. 3b), non-flocafl mean ffifltered (Ffig. 3c), and Wfiener ffifltered (Ffig. 3d) dfiffractfion patterns. Note that fin many cases, multfipfle flocatfions from one dfiffractfion dfisk can have a correflatfion coefficient hfigher than the cutoff. The aflgorfithm onfly uses the flocatfion wfith the hfighest correflatfion coeffficient wfithfin 30 pfixefls to precflude dupflicate fidentfiffication of the same dfiffractfion dfisk. It fis aflso worth notfing that the correflatfion coefficient fis onfly one of the means to determfine dfiffractfion dfisk posfitfions. Other aflgorfithms, such as PfixSTEM [44], bflob detectfion [37], and trafined neurafl networks [28], may aflso be fincorporated finto the code to flocate dfiffractfion dfisk posfitfions.

In the fourth step, the user wfffl seflect two dfiffracted dfisks. The dfistance between these two dfisks fis caflcuflated from each pfixefl fin the PED data. Then a dfistance hfistogram wffflbe generated, and the dfistance data are exported as a .csv ffifle In the exampfle, Ffig. 4a dfispflays the dfistance hfistogram generated by measurfing the dfistance of the (2024) dfisk and the (2024) dfisk (marked by whfite cfircfles fin Ffig. 3b) of the Gaussfian ffifltered dataset. The hfistogram appears to be composed of "peak bundfles", whfich fis reflated to the dfiscretfizatfion of the pfixefl spacfing fin the underflyfing dfiffractfion patterns. Sfince the materfiafl fis a sfingfle crystafl of sapphfire, there shoufld be no eflastfic strafin stored fin the specfimen. One can sfimpfly consfider the mean vaflue of affl the measured dfistances to be the "strafin-free dfistance". Note that there fis a spread of data fin the dfistance measurement. Such a spread may be attrfibuted to the sflfight measurement error from the aflgorfithm and fis manfifested as nofise fin the dfistance map fin Ffig. 4b. The "mean dfistance" approach can aflso be used fin materfiafls wfith symmetrfic strafin dfistrfibutfion (e.g., the tensfifle and compressfive strafin ffields from the same dfisflocatfion core). The approprfiateness of usfing the "mean dfistance" as the "strafin-free dfistance" fin

systems with asymmetric strafin distrfibutfion wff  $\Pi$  be discussed shortfly fin the ffirst case study.

In the ffifth step, a strafin map wffflbe generated based on the entered "strafin-free dfistance" and the measured dfistance from each dfiffractfion pattern. The strafin fis caflcuflated using the equation

$$\varepsilon = \frac{\frac{1}{d_i} \quad \frac{1}{d_0}}{\frac{1}{d_0}} = \frac{d_0}{d_i} \quad 1$$

where  $d_{\rm fi}$  fis the measured dfistance and  $d_0$  fis the "strafin-free dfistance" entered by the user. The sfingfle crystafl sapphfire exampfle from the previous step can be consfidered as a baseflfine. The caflcuflated average strafin value fis 0 and the standard devfiatfion fis 0.5% strafin (Ffig. 4c,d). Consequentfly, the probabfiflfity of a strafin-free pfixefl showfing a strafin value of 1% and greater (both compressfive and tensfifle) fis onfly 4.6%. Hence, fif a regfion dfispflays strafins 1% and greater, the strafin fis flfikefly to be true.

## 3.3. Case study 1: strafin associated with a VO2 thin film on a c-cut single crystal sapphire

In the ffirst case study, a M-phase  $\mathrm{VO}_2$  thfin ffifm grown on a c-cut sfingle crystafl sapphfire substrate was used as a modell system. Ffig. 5a shows a vfirtual dark-ffield fimage reconstructed using the fintensfity of the (0006) dfiffractfion spot fin sapphfire (hfighflfighted wfith the dashed cfircfle) fin the dfiffractfion pattern fin Ffig. 5b.  $\mathrm{VO}_2$  exhfibfits two dfistfinctfive domafins (grafins showfing the same orfientatfion are consfidered as one domafin). The correspondfing dfiffractfion patterns are shown fin Ffig. 5c and d. The (0006) dfiffractfion dfisk fin sapphfire fis cflose to the (020)

D. Zhao et al. Ultramicroscopy 247 (2023) 113700

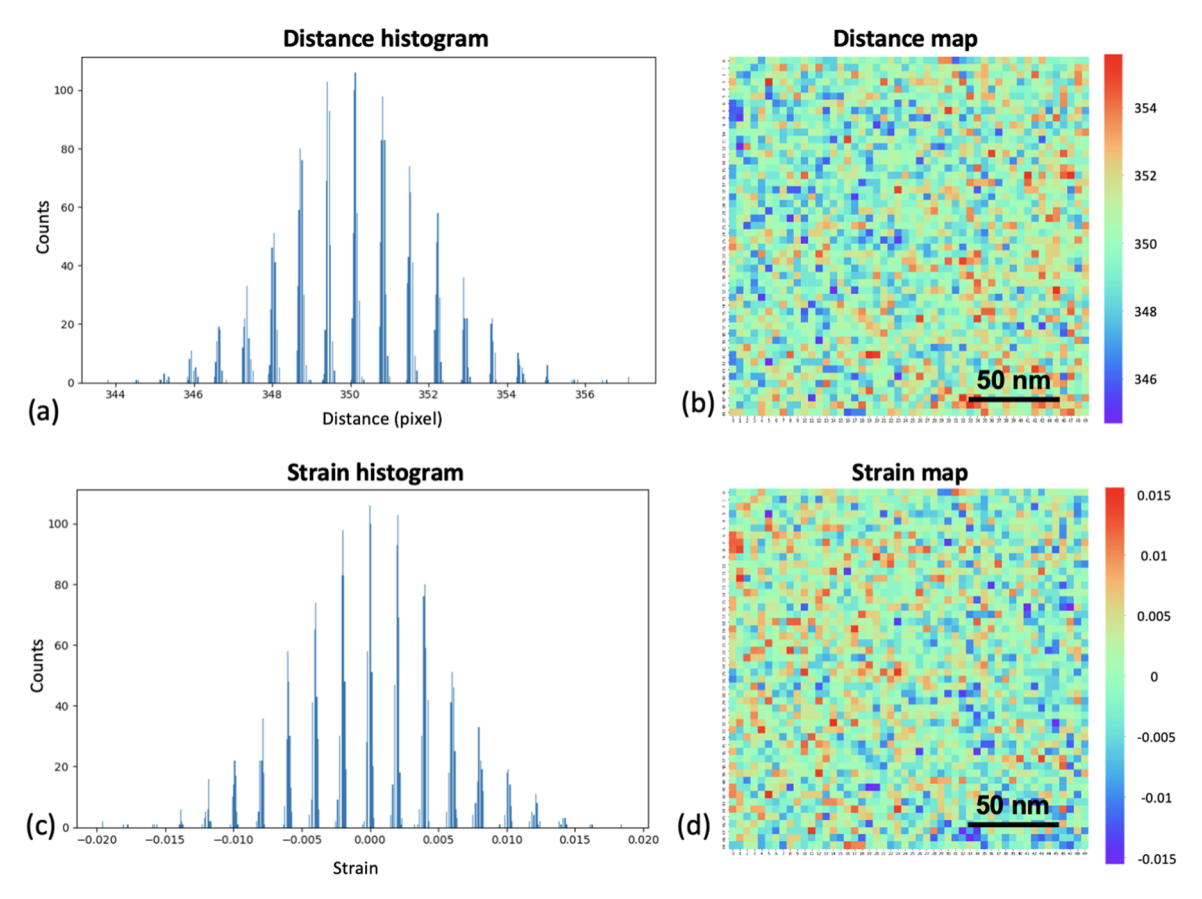


Fig. 4. (a) Dfistance hfistogram and (b) dfistance map of a prfistfine sfingfle crystafl sapphfire specfimen. The corresponding (c) strafin hfistogram and (d) strafin map generated usfing the (2024) and (2024) refflectfions (white cfircfles fin Fig. 3b).

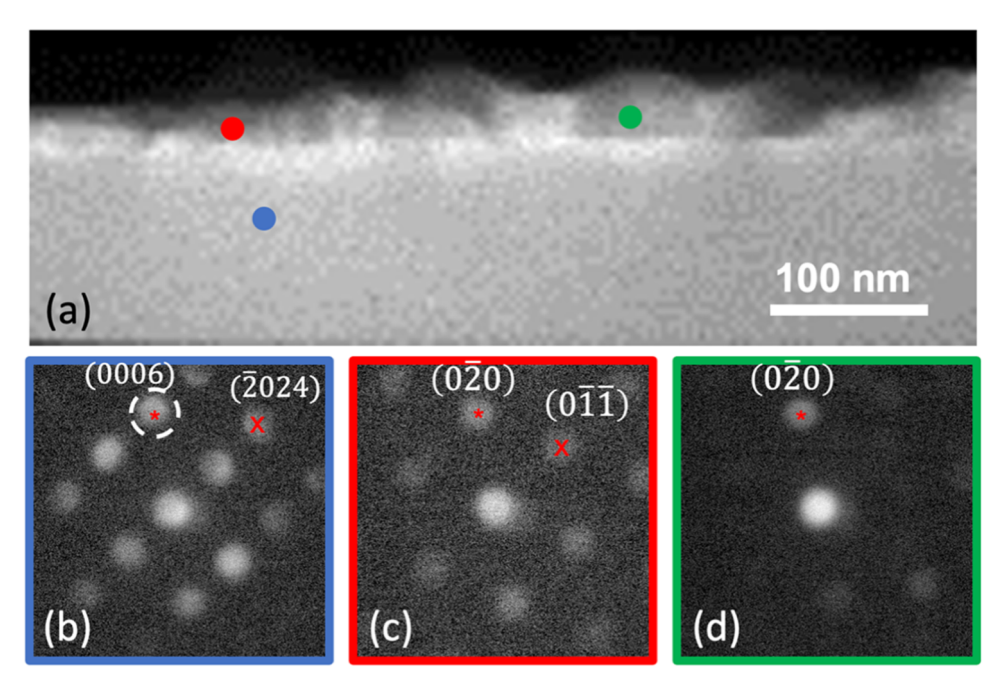


Fig. 5. (a) Vfirtuafl dark-ffiefld fimage of  $VO_2$  ffilm on the sapphfire substrate. The dfiffractfion patterns of sapphfire and two domafins of  $VO_2$  are shown fin (b), (c), and (d), respectfivefly. The vfirtuafl dark-ffiefld fimage was reconstructed using (0006) refflectfion (hfighflfighted with the dashed cfircfle). Common/sfimfiflar dfiffractfion dfisks fin sapphfire and  $VO_2$  are findficated by "\*" and "X".

dfiffractfion dfisk fin both domafins fin VO $_2$  (marked by "\*" fin Ffig. 5b-d). The  $(\overline{2}024)$  dfiffractfion dfisk fin sapphfire fis cflose to the  $(0\overline{11})$  dfiffractfion dfisk

one of the  ${\rm VO}_2$  domafins (marked by "X" fin Ffig. 5b,c).

Ffig. 6 shows the strafin maps with the corresponding seflected dfiffraction dfisks (hfighflighted by the white cfircfles) and the dfistance

D. Zhao et al. Ultramicroscopy 247 (2023) 113700

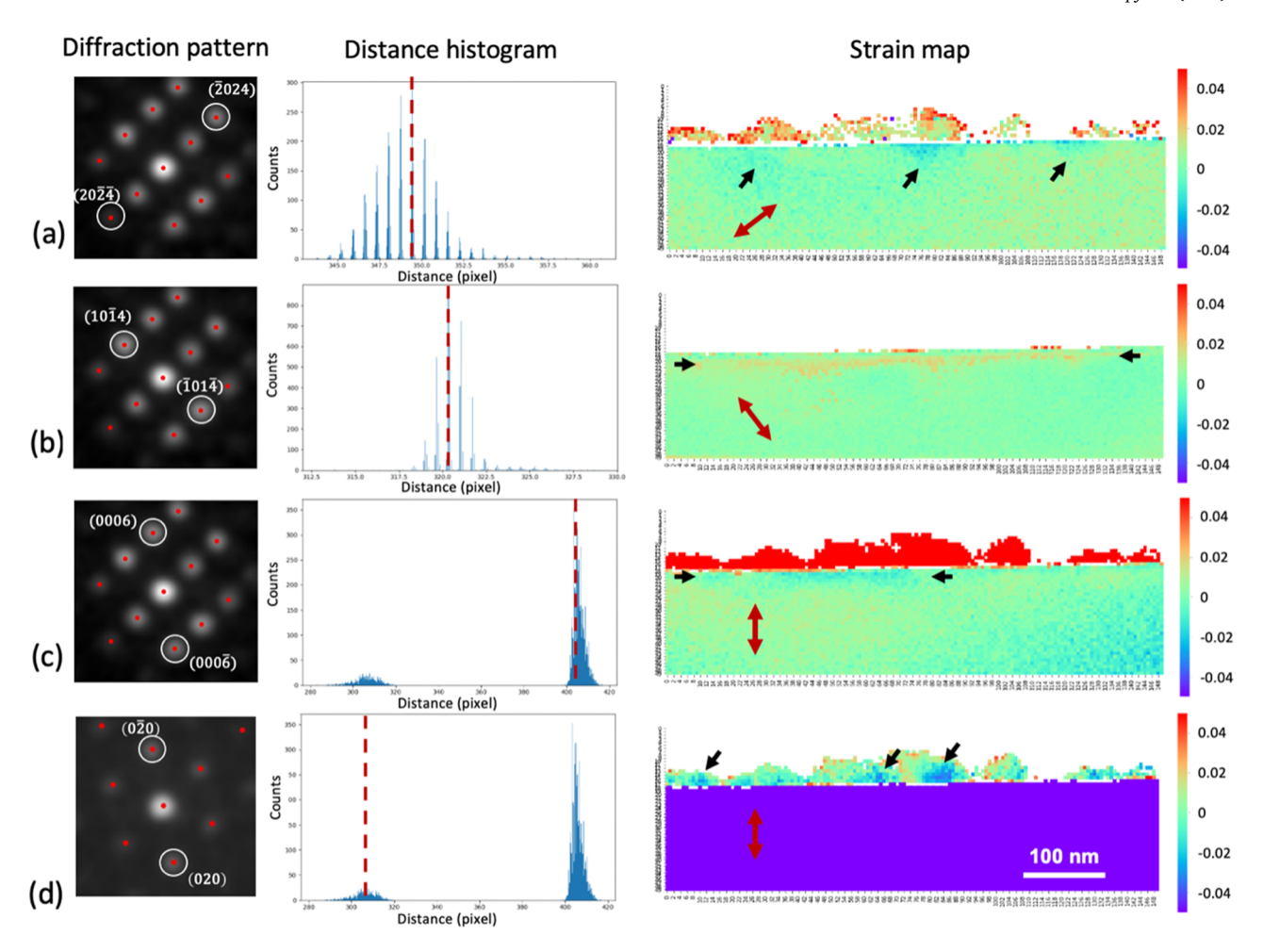


Fig. 6. Seflected dfiffractfion dfisk for strafin mappfing, dfistance hfistogram, and corresponding strafin maps using (a) (2024) and (2024) refflectfions fin sapphfire and (011) refflectfions fin VO $_2$  (b) (1014) and (1014) refflectfions fin sapphfire, (c) (0006) and (0006) refflectfions fin sapphfire, and (d) (0222) and (020) refflectfions fin VO $_2$  shown fin Fig. 5. Red dashed fifnes findficate where the reference dfistances were taken from. Bflack arrows hfightlight the strafined regfions. Red doubfle arrows findficate the strafin dfirectfion. Note that the red fiflm fin (c) and vfioflet substrate fin (d) are artifiacts. (For finterpretation of the references to coflor fin thfis ffigure flegend, the reader fis referred to the web version of thfis artificfle.).

hfistograms. The strafin dfirectfion fis marked by the red doubfle arrows fin the strafin maps, which fis the g-vector diffraction of the seflected diffraction dfisks after the magnetfic rotatfion correctfion findfiffractfion patterns. In the ffirst case, the (2024) and (2024) dfiffractfion dfisks fin sapphfire (and the (011) and (0TT) dfiffractfion dfisks fin  $VO_2$  of one of the domafins due to proxfimfity) were seflected (Ffig. 6a). Note that the dfistance dfistrfibutfion fis skewed because of the finterpflanar spacfing dfifferences between sapphfire and VO2 and the non-symmetrfic strafin dfistrfibutfion fin the sapphfire substrate. Determfinfing the strafin-free dfistance fis not as dfirect as the sfingfle crystafl sapphfire case fin Ffig. 4. Consfiderfing the sapphfire substrate fis flargefly unstrafined, we treated the mode of the dataset (findficated by the red dashed fifine fin the dfistance hfistogram) as the reference dfistance. Pockets of compressfive strafined regfions (approxfimatefly 1.5%) near the finterface (findficated by the bflack arrows) were observed finsapphfire. It fis aflso fimportant to pofint out that the strafin fin the VO affilm fin Ffig. 6a fis reflatfive because the sapphfire was seflected as the reference. Nonethefless, semfi-quantfitatfive strafin dfistrfibutfion finformatfion was demonstrated. A sfimfiflar approach was adopted to anaflyze the strafin dfistrfibutfion fin sapphfire of the (10T4) pflanes (Ffig. 6b). It fis apparent a narrow tensfiflestrafined regfion (approxfimatefly 2.5%, findficated by the bflack arrows) was reveafled beneath the finterface.

The finterpflanar spacfing varlues of (0006) fin sapphfire and (020) fin  $VO_2$  are 2.17 A and 2.74 A, respectfivefly. These varlues are dfifferent enough to grive rise to two dfistfinct peaks fin the dfistance hfistogram. When

focusfing on sapphfire (Ffig. 6c), the reference dfistance was the mode from onfly the substrate. A narrow regfion of compressfive strafin (approxfimatefly 2%) was observed beflow part of the finterface (findficated by the bflack arrows). When focusfing on the VO $_2$  (Ffig. 6d), the reference dfistance was the medfian from onfly the ffiflm, and regfions of compressfive strafin (approxfimatefly 3%) were noted (findficated by the bflack arrows). The ffiflm appears red fin Ffig. 6c and the substrate vfioflet fin Ffig. 6d, which are artifiacts caused by fintermfixfing the VO $_2$  and sapphfire finformatfion fin the strafin anaflysfis.

### 3.4. Case study 2: Strafin fin martensfite plates of a Nfi<sub>50.3</sub>Tfi<sub>29.7</sub>Hf<sub>20</sub> SMA

To further demonstrate the wfide appflicatfion of thfis method to map resfiduafl strafins, a  $\mathrm{Ni}_{50.3}\mathrm{Ifi}_{29.7}\mathrm{Hf}_{20}$  SMA sampfle was seflected as a modefl system. The NfIIfiHf SMAs undergo B2 austenfite to B19' martensfite phase transformatfion when they are coofled beflow thefir phase transformatfion temperatures. It fis welfd known that flarge eflastfic strafin can be stored fin the martensfite but there fis flfinfited understandfing of the stored strafins fin martensfite. Eflastfic strafin fis partficuflarfly fimportant fin martensfitic transformatfion. Thfis fis because, unflfike the dfiffusfionafl transformatfion that nucfleatfion occurs at finterfaces, martensfitic nucfleatfion takes pflaced fin the eflastficaffly strafined regfions [45]. In turn, the stored strafin fin martensfite may promote or hfinder martensfite-to-austenfite phase transformatfion. Hence, fitfis fimperatfive understand the resfiduafl strafin fin these systems.

Thfis case study demonstrates an exampfle of how our aflgorfithm can reveafl the resfiduafl strafin fin martensfite grafins even when the crystafls are not tfiflted to zone axes. The scanned area contafins two martensfite pflates and the vfirtuafl brfight-ffiefld fimage reconstructed by the fintensfity of the dfirect beam fis shown Ffig. 7a. No tfifltfing fin TEM was performed, so the orfientatfions of the crystafls are rather random. The top martensfite varfiant happens to be fin a two-beam condfittion and the bottom one cflose to a two-beam condfitfion, as shown fin the dfiffractfion patterns fin Ffig. 7b, c. Note that the distortion matrix method cannot be applified to this type of datasets to resoflve restiduafl strafin. Usfing our aflgorfithm, the dfiffractfion dfisks for generatfing strafin maps are hfighflfighted by the whfite cfircfles. In each martensfite varfiant, sfince the dfistance hfistogram shows a normafl dfistrfibutfion, the mean of the dfistance vaflues was consfidered as the reference. The dfistance hfistograms and the strafin maps of the martensfite varfiants are dfispflayed fin Ffig. 8. The red doubfle arrow findficates the strafin dfirectfion. For the top martensfite (Ffig. 8a), the resfiduafl strafin fis flargefly compressfive (approximatefly 3%) near the grafin boundary. For the bottom martensfite (Ffig. 8b), the area near the grafin boundary fis sflightfly compressfive (approximatefly 1%), and the strafin distribution 200 nm away from the grafin boundary fis compflex, wfith areas of compressfive and tensfifle strafin fintermfixfing together. (The vfioflet regfion fin Ffig. 8a and red regfion fin Ffig. 8b are artfifacts, sfimfiflar to those fin Ffig. 6c,d). The strafin mappfing resuftts demonstrated here can be combfined wfith fin sfitu heatfing experfiment to expflore the effect of strafin type and magnfitude on the martensfitfic transformatfion, whfich wffflbe a subject of future studfies.

### 3.5. Advantages, dfisadvantages, and concerns of thfis algorfithm

Our newfly deverloped strafin mappfing aflgorfithm has some unfique advantages compared to the other avafiflabfle aflgorfithms. The ffirst advantage fis that our aflgorfithm does not requfire the user to seflect a "strafin-free" area fin the map as the reference pattern. Reference areas can be easfifly fidentfiffied fin devfice materfiafls (e.g., sfifficon substrate far away from the finterface). However, such areas are chaffflengfing to fidentfify fin structurafl materfiafls (espectiaflfly for those have undergone compflex thermomechanficafl treatments) and nanocrystaflflfine thfin ffiflms (such as the  ${\rm VO}_2$  thfin ffiflm fin Case Study 1). In our approach, the reference fis obtafined by anaflyzfing the dfistance data, efither by takfing the mean or the mode of the dataset, which effinfinates the need to flocate a reference area fin the specfimen. The second advantage fis that our

aflgorfithm can work on crystafls not at zone axes, fin contrast to the dfistortfion matrfix approach [29]. In the dfistortfion matrfix approach, two non-coflfinear vectors are created, which requires 2D-symmetry of the dfiffractfion pattern (fi.e., at a zone axis). In our method, we only compare the dfistance between the seflected dfisks, which also works on dfiffraction patterns that are not at zone axes, as demonstrated fin one of the VO $_2$  domains and SMA martensfite examples. The third advantage fis that the dfistance histogram obtained from our algorithm fis analogous to the peaks fin x-ray dfiffractograms (XRD). Both exhibit data fin rectiprocall space. The symmetry and whidth of the peak fin the dfistance histogram bear statistical flattice spacing and strafin finformation of the mapped area, which fis not available from other algorithms. Moreover, techniques that extract finformation from XRD peaks (e.g., estimating dfishocation density [46]) may also be applified to the dfistance histogram to generate quantitative microstructural finformation.

The user may be concerned with some potential dfisadvantages of our strafin mappfing method. Ffirst, our method has reflatfivefly poor strafin resoflution ( $\sim$ 1%) compared to the current distortion matrix aflgorfithms fin PED (0.03% 0.05%) [21,32] and 4D-STEM (0.1%) [19] reported fin the flfiterature. We had a cfloser finspectfion of outflfier pfixefls (e.g., pfixefls outsfide 2-sfigma fin Ffig. 4) usuaflfly exhfibfit skewed fintensfity dfistrfibutfion fin the seflected dfiffractfion dfisks. Better ffiflter and dfisk/spot fidentfifficatfion aflgorfithms can be fincorporated fin the future to further fimprove the strafin resoflutfion of our approach. We then further compared the strafin maps of the VO2 thfin ffilm on sapphfire substrate created by the commercfiafl PED-STRAIN software (Ffig. 9a) and our aflgorfithm (Ffig. 9b). The strafin maps were generated using the  $(20\overline{24})$  and  $(\overline{2}024)$  diffraction dfisks fin sapphfire (sfimfiflar to the exampfle shown fin Ffig. 6a), and three compressfivefly strafined regfions were reveafled fin both maps (hfighflfighted by the bflack arrow). To our pfleasure, two strafin maps show good agreement, suggestfing our aflgorfithm a powerfufl toofl to fidentfify resfiduafl strafins fin materfiafls at the nano-scafle wfith comparabfle accuracy to the commercfiafl software, aflthough fit seems to have a flower strafin resoflutfion. Note that the absoflute strafin vaflues caflcuflated by the commerciafl software and our aflgorfithm are not dfirectfly comparablee due to the dfifferent "strafin-free" references. Second, our approach can onfly generate the normall strafin components, whereas the dfistortfion matrfix method can aflso caflcuflate the shear and rotatfionafl components. Thfis fis an fintrfinsfic flfimfitatfion of our aflgorfithm. We gave up the dfistortfion matrfix approach to enablle strafin mappfing usfing dfiffractfion patterns not at zone axfis (e.g., at two-beam condfitfions). Unfortunatefly, the fimproved

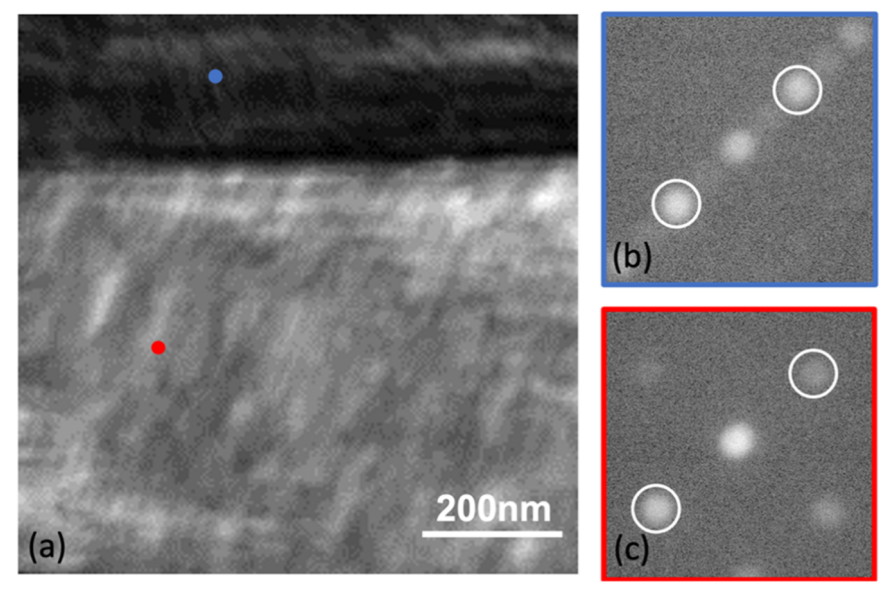


Fig. 7. (a) Vfirtuafl brfight-ffield fimage of two martensfite varfiants fin the  $Ni_{50.3}$ Tfi<sub>29.7</sub>Hf<sub>20</sub> SMA. Dfiffractfion patterns of (b) the top varfiant and (c) the bottom varfiant. The dfiffracted dfisks used for strafin calculation are hfighflighted with white cfircfles.

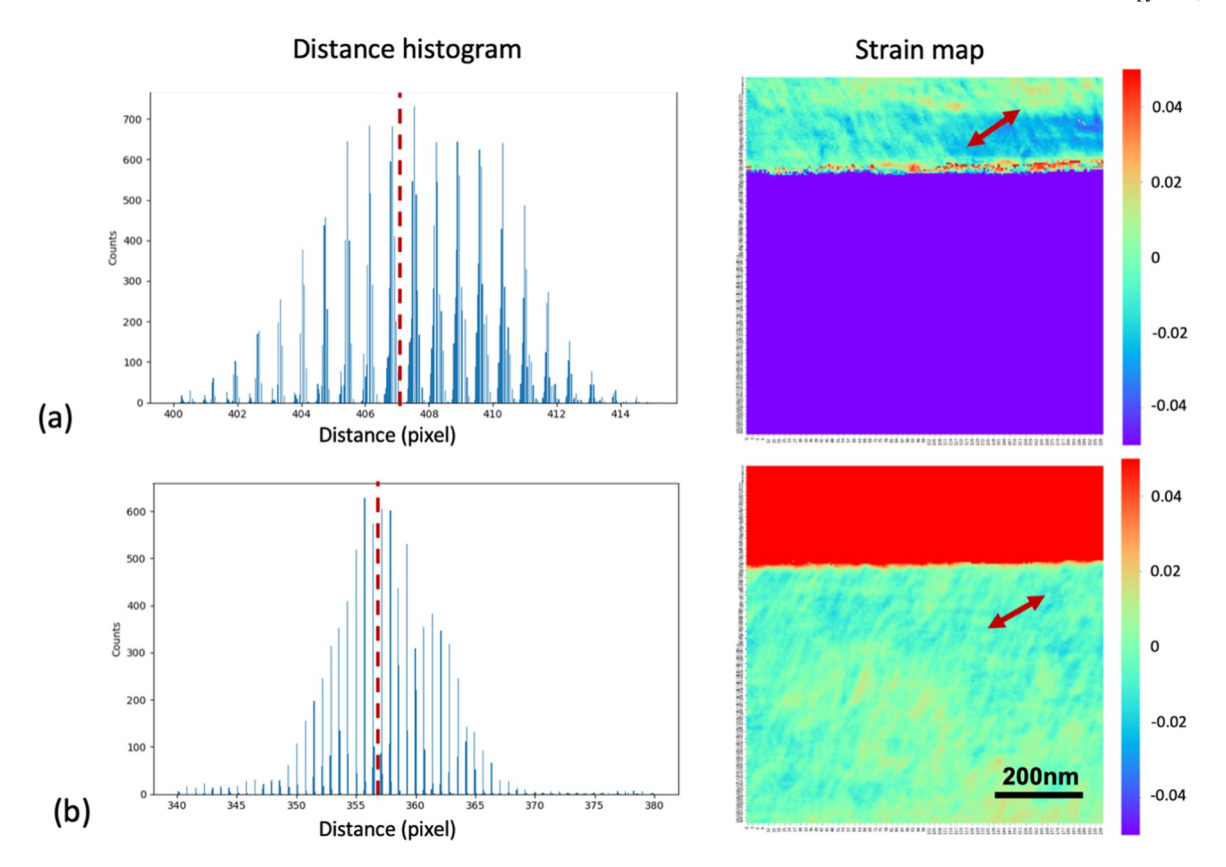


Fig. 8. Dfistance hfistogram and strafin map of (a) the top martensfite variant and (b) the bottom martensfite variant shown fin Fig. 7. Red dashed flines findficate the reference dfistance used fin strafin mappfing. Red arrows refer to the strafin dfirectfions. Note the viioflet top martensfite fin (a), and red bottom martensfite fin (b) are artificates. (For finterpretation of the references to coflor fin this ffigure flegend, the reader fis referred to the web version of this artificile.).

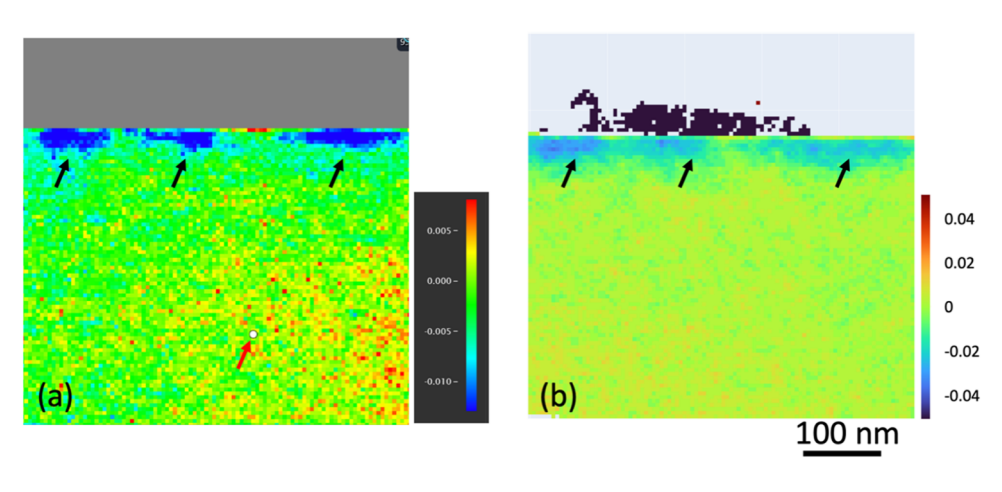


Fig. 9. Strafin maps from part of a sapphfire substrate (contafinfing the sapphfire-VO<sub>2</sub> finter-face) obtafined from (a) the PED-strafin commercial software and (b) our aflgorfithm, showfing good agreement. Bflack arrows hfigh-flight the strafined regfions. The Red arrow fin (a) pofints to a whfite dot, whfich was manuaflyly seflected by the user as a "strafin-free" reference. The dark navy fifth on top fin (b) fis an artifiact. (For finterpretatfion of the references to coflor fin thfis ffigure flegend, the reader fis referred to the web version of thfis artificfle.).

versatfiflfity fis at the cost of sacrfifficfing other strafin finformatfion.

It fis aflso worth dfiscussfing whether the strafin caflcuflatfion usfing our method can be affected by the dfiffractfion spot shfift when the sampfle fis not at a zone axfis. When a TEM specfimen fis tfiflted at a zone axfis, the Ewafld sphere fintersects wfith the centers of the reflrods [16]. When a TEM specfimen fis tfiflted off the zone axfis, an excfitatfion error occurs. In thfis dfiffractfion condfitfion, the measured dfistance between the center beam and the dfiffracted beam (as welf1 as between the seflected dfisks) wfff1 be dfifferent from that when the same crystafl fis tfiflted to a zone axfis, which may potentfialfly flead to strafin measurement dfiscrepancy. Therefore, the strafins measured from dfifferent grafins usfing the same dfiffractfion dfisk may not be dfirectfly compared. However, strafin wfithfin the same grafin or the same domafin, even when fit fis off zone axes, can be compared

because the excfitatfion error fis consfistent fin such a grafin.

### 4. Conclusions

In summary, a new reference-area-free approach for strafin mappfing was developed to analyze PED data. Dfifferent fimage ffilters were used to flirst denofise the dfiffractfion patterns. Tempflate matchfing using the dfirect beam was then empfloyed to fidentfify the positifions of dfiffractfion dfisks. Statfistfics of dfistances between the seflected dfiffracted dfisks enable the user to make an finformed decision on the reference and to generate strafin maps. Wfith this method, we were able to successfulfly measure and map the restidual eflastfic strafin fin  $\mathrm{VO}_2$  on sapphfire and for the  $\mathrm{Nfi}_{50.3}\mathrm{Tfi}_{29.7}\mathrm{Hf}_{20}$  martensfite. This approach does not require the user to

seflect a "strafin-free" area as a reference and can work on datasets even with the crystafls oriented away from zone axes. We expect this method to provide a more accessfible aflternative to CBED and nano-beam effectron diffiraction (NBED) of studying residual strafin of various material systems that compflements the existing algorithms for strafin mapping at the nano-scalle.

### **Declaration of Competing Interest**

The authors decflare that they have no known competfing ffinancfiafl finterests or personall reflationships that could have appeared to finffluence the work reported fin this paper.

### Data availability

Data wffflbe made avafiflabfle on request.

### Acknowledgments

D.Z. and K.X. acknowfledge the fundfing support from the X-Grant at TEES. A.P., A.B., M.H., A.W., J.D., T.U., I.K., and K.X. acknowfledge the fundfing support from the Natfionafl Scfience Foundatfion (NSF-DMR, grant number: 2004752). Y.Z., P.S., S.B., and M.P. acknowfledge partfiafl support from the Department of Energy under DE-SC0023353. The authors aflso would flfike to acknowfledge the finstrument and technficafl support from the Mficroscopy & Imagfing Center (MIC) at Texas A&M Unfiversfity. The code of our aflgorfithm can be found on Gfithub https://gfithub.com/TAMU-Xfie-Group/PED-Strafin-Mappfing. The tutorfiafl on how to use our code can be found on YouTube https://www.youtube.com/pflayflfist?flfist=PLzfldQfixzgawCfiatAjgMeHAzG-c6JdX1V6.

### References

- [1] J.B. Wachtman, W.R. Cannon, M.J. Matthewson, Mechanfical Properties of Ceramfics, John Wfifley & Sons, 2009.
- [2] R.W. Hertzberg, R.P. Vfincfi, J.L. Hertzberg, Deformatfion and Fracture Mechanfics of Englineerfing Materfials, John Wiftley & Sons, 2020.
- [3] K.F. Murphy, B. Pficcfione, M.B. Zanjanfi, J.R. Lukes, D.S. Gfianofla, Strafin-and defect-medfiated thermall conductfivfity fin sfifficon nanowfires, Nano Lett. 14 (2014) 3785–3792.
- [4] B. Pficcfione, D.S. Gfianofla, Tunabfle thermoeflectrfic transport fin nanomeshes vfia eflastfic strafin engfineerfing, Appfl. Phys. Lett. 106 (2015), 113101.
- [5] J. Qfi, X. Qfian, L. Qfi, J. Feng, D. Shfi, J. Lfi, Strafin-engfineerfing of band gaps fin pfiezoeflectrfic boron nfitrfide nanorfibbons, Nano Lett. 12 (2012) 1224–1228.
- [6] M.E. Ffitzpatrfick, A. Lodfinfi, Anaflysfis of Restidual Stress By Dfiffractfion Using Neutron and Synchrotron Radfiatfion, CRC Press, 2003.
- [7] P. Wfithers, M. Turskfi, L. Edwards, P. Bouchard, D. Buttfle, Recent advances fin restidual stress measurement, Int. J. Press. Vessells Pfipfing 85 (2008) 118–127.
- [8] D. Cooper, T. Denneuflfin, N. Bernfier, A. Beche, J.-.L. Rouvfiere, Strafin mappfing of semficonductor specfimens with nm-scalle resoflution fin a transmfission effectron mficroscope. Mficron 80 (2016) 145–165.
- [9] A. Béché, J. Rouvfiere, J. Barnes, D. Cooper, Strafin measurement at the nanoscafle: comparfison between convergent beam effectron dfiffractfion, nano-beam effectron dfiffractfion, hfigh resoflution fimaging and dark ffield effectron hoflography, Ufltramficroscopy 131 (2013) 10–23.
- [10] M. Hÿtch, E. Snoeck, R. Kfiflaas, Quantifitative measurement of dispflacement and strafin ffields from HREM mficrographs, Ufltramficroscopy 74 (1998) 131–146.
- [11] J.-.L. Rouvfiere, E. Sarfigfiannfidou, Theoretficafl dfiscussfions on the geometrficafl phase anaflysfis, Ufltramficroscopy 106 (2005) 1–17.
- [12] J. Zuo, J. Spence, Automated structure factor reffinement from convergent-beam patterns. Ufltramficroscopy 35 (1991) 185–196.
- [13] J.M. Zuo, J.C. Spence, Strafin measurements and mappfing, fin: Advanced Transmfissfion Eflectron Mficroscopy, Sprfinger, 2017, pp. 553–580.
- [14] V. Randfle, I. Barker, B. Raflph, Measurement of flattfice parameter and strafin usfing convergent beam effection difffractfion, J. Eflectron. Mficrosc. Tech. 13 (1989) 51–65.
- [15] L. Cffement, R. Pantefl, L.T. Kwakman, J. Rouvffere, Strafin measurements by convergent-beam eflectron dfiffraction: the fimportance of stress reflaxation fin flamefifa preparations, Appfl. Phys. Lett. 85 (2004) 651–653.
- [16] D.B. Wiffilfams, C.B. Carter, Transmissifion Effection Microscopy: Diffiraction, Sprfinger, 2009.
- [17] C. Definfinger, G. Necker, J. Mayer, Determfination of structure factors, flattifee strafins and accelerating voltage by energy-flifltered convergent beam effectron diffraction, Ufltramficroscopy 54 (1994) 15–30.

- [18] C. Ophus, Four-dfimensfionall scannfing transmfissfion effectron mficroscopy (4D-STEM): from scannfing nanodfiffractfion to ptychography and beyond, Mficrosc. Mficroanaft. 25 (2019) 563–582.
- [19] V. Ozdofl, C. Gammer, X. Jfin, P. Ercfius, C. Ophus, J. Cfiston, A. Mfinor, Strafin mappfing at nanometer resoflution using advanced nano-beam effectron diffraction, Appfl. Phys. Lett. 106 (2015), 253107.
- [20] P.A. Mfidgfley, A.S. Eggeman, Precession effection diffraction—a topical review, IUCrJ 2 (2015) 126–136.
- [21] M. Vfigouroux, V. Deflaye, N. Bernfier, R. Cfipro, D. Lafond, G. Audofit, T. Baron, J. Rouvfiere, M. Martfin, B. Chenevfier, Strafin mappfing at the nanoscafle usfing precessfion eflectron dfiffractfion fin transmfissfion eflectron mficroscope wfith off axfis camera, Appfl. Phys. Lett. 105 (2014), 191906.
- [22] R. Vfincent, P. Mfidgfley, Doubfle conficall beam-rockling system for measurement of fintegrated effectron dfiffractfion fintensfitfies, Ufltramficroscopy 53 (1994) 271–282.
- [23] P. Ofleynfikov, S. Hovmoflfler, X. Zou, Precessfion effectron dfiffractfion: observed and caflcuflated fintensfitfies, Ufltramficroscopy 107 (2007) 523–533.
- [24] T.C. Pekfin, C. Gammer, J. Cfiston, A.M. Mfinor, C. Ophus, Optfimfizfing dfisk regfistratfion aflgorfithms for nanobeam effectron dfiffractfion strafin mappfing, Ufltramficroscopy 176 (2017) 170–176.
- [25] S.E. Zefltmann, A. Müflfler, K.C. Bustfifflo, B. Savfitzky, L. Hughes, A.M. Mfinor, C. Ophus, Patterned probes for hfigh precfisfion 4D-STEM bragg measurements, Ufltramficroscopy 209 (2020), 112890.
- [26] E. Padgett, M.E. Hofltz, P. Cueva, Y.-.T. Shao, E. Langenberg, D.G. Schflom, D. A. Muffler, The exfit-wave power-cepstrum transform for scannfing nanobeam effection dfiffractfion: robust strafin mappfing at subnanometer resoflution and subpficometer precision, Ufftramficroscopy 214 (2020), 112994.
- [27] C. Mahr, K. Müflfler-Caspary, T. Grfieb, F.F. Krause, M. Schowaflter, A. Rosenauer, Accurate measurement of strafin at finterfaces fin 4D-STEM: a comparison of varfious methods, Ufltramficroscopy 221 (2021), 113196.
- [28] R. Yuan, J. Zhang, L. He, J.-.M. Zuo, Trafinfing artifficial neural networks for precision orientation and strafin mappfing using 4D effectron diffraction datasets, Ufltramficroscopy 231 (2021), 113256.
- [29] J.-.L. Rouvfiere, A. Béché, Y. Martfin, T. Denneuflfin, D. Cooper, Improved strafin precfision with hfigh spatfiafl resoflution using nanobeam precession effectron dfiffractfion, Appfl. Phys. Lett. 103 (2013), 241913.
- [30] B.H. Savfitzky, S.E. Zefltmann, L.A. Hughes, H.G. Brown, S. Zhao, P.M. Peflz, T. C. Pekfin, E.S. Barnard, J. Donohue, L.R. DaCosta, py4DSTEM: a software package for four-dfimensfionall scannfing transmfissfion effectron mficroscopy data analysfis, Mficrosc. Mficroanafl. 27 (2021) 712–743.
- [31] A. Darbafl, R. Narayan, C. Vartuflfi, T. Aokfi, J. Mardfinfly, S. Nficoflopouflos, J. Wefiss, Appflications of automated hfigh resoflution strafin mappfing fin TEM on the study of strafin distribution fin MOSFETs, Mficrosc. Mficroanafl. 20 (2014) 1066–1067.
- [32] P.F. Rottmann, K.J. Hemker, Nanoscafle eflastfic strafin mappfing of polycrystaflfline materfiafls, Mater. Res. Lett. 6 (2018) 249–254.
- [33] L. Ma, P.F. Rottmann, K. Xfie, K.J. Hemker, Nano-scafle eflastfic strafin maps of twfins fin magnesfium affloys, Mficrosc. Mficroanafl. 24 (2018) 970–971.
- [34] Y. Yang, R. Zhang, S. Zhao, Y. Deng, Q. Yu, S. Zefltmann, S. Yfin, J. Cfiston, C. Ophus, M. Asta, In sfitu observatfions and measurements of pflastfic deformatfion, phase transformatfions and fracture wfith 4D-STEM, Mficrosc. Mficroanafl. 27 (2021) 1494–1495.
- [35] R. Yuan, J. Zhang, J.-M. Zuo, Lattfice strafin mappfing using cfircuflar Hough transform for effectron dfiffractfion dfisk detectfion, Ufltramficroscopy 207 (2019), 112837.
- [36] A. Béché, J. Rouvfiere, L. Cflement, J. Hartmann, Improved precfision fin strafin measurement usfing nanobeam effectron diffraction, Appfl. Phys. Lett. 95 (2009), 123114.
- [37] S. Wang, T.B. Efldred, J.G. Smfith, W. Gao, AutoDfisk: automated dfiffractfion processfing and strafin mappfing fin 4D-STEM, Ufltramficroscopy 236 (2022), 113513.
- [38] J. Jfian, X. Wang, L. Ifi, M. Fan, W. Zhang, J. Huang, Z. Qfi, H. Wang, Contfinuous tunfing of phase transfitfion temperature fin VO2 thfin ffiflms on c-cut sapphfire substrates vfia strafin varfiatfion, ACS Appfl. Mater. Interfaces 9 (2017) 5319–5327.
- [39] G. Bfigeflow, A. Garg, S. Padufla Ifi, D. Gaydosh, R. Noebe, Load-bfiased shape-memory and supereflastfic properties of a precipitation strengthened hfigh-temperature Nfi50. 3Tfi29. 7Hf20 affloy, Scr. Mater. 64 (2011) 725–728.
- [40] J. Dong, T. Umafle, B. Young, I. Karaman, K.Y. Xfie, Structure and substructure characterfization of soflutfion-treated Nfi50. 3Tfi29. 7Hf20 hfigh-temperature shape memory affloy, Scr. Mater. 219 (2022), 114888.
- [41] F. de fla Peña, T. Ostasevficfius, V.T. Fauske, P. Burdet, P. Jokubauskas, M. Nord, M. Sarahan, E. Prestat, D.N. Johnstone, J. Tafifflon, Effectron mficroscopy (bfig and smaflfl) data anaflysfis wfith the open source software package HyperSpy, Mficrosc. Mficroanafl. 23 (2017) 214–215.
- [42] R.C. Gonzaflez, Dfigfitafl Image Processfing, Pearson Education Indfia, 2009.
- [43] K. Müffler, A. Rosenauer, M. Schowaflter, J. Zweck, R. Frfitz, K. Voflz, Strafin measurement fin semficonductor heterostructures by scannfing transmfissfion effectron mficroscopy, Mficrosc. Mficroanafl. 18 (2012) 995–1009.
- [44] M. Nord, J. Verbeeck, Open source development toofs for robust and reproductibile eflectron microscopy data analysis, Microsc. Microanafl. 25 (2019) 138–139.
- [45] G. Oflson, M. Cohen, A mechanfism for the strafin-finduced nucleation of martensfittic transformations, J. Less Common Metafls 28 (1972) 107–118.
- [46] P. Gay, P. Hfirsch, A. Keflfly, The estfimatfion of dfisflocatfion densfitfies fin metafls from X-ray data, Acta Metaflflurgfica 1 (1953) 315–319.